NASA/TM-2001-211243

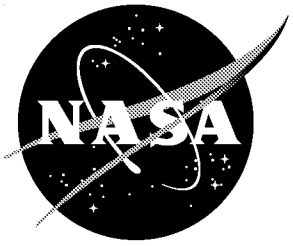

System Identification and Pod Method Applied to Unsteady Aerodynamics

Deman Tang and Denis Kholodar
Duke University, Durham, North Carolina

Jer-Nan Juang
Langley Research Center, Hampton, Virginia

Earl H. Dowell
Duke University, Durham, North Carolina

December 2001

The NASA STI Program Office ... in Profile

Since its founding, NASA has been dedicated to the advancement of aeronautics and space science. The NASA Scientific and Technical Information (STI) Program Office plays a key part in helping NASA maintain this important role.

The NASA STI Program Office is operated by Langley Research Center, the lead center for NASA's scientific and technical information. The NASA STI Program Office provides access to the NASA STI Database, the largest collection of aeronautical and space science STI in the world. The Program Office is also NASA's institutional mechanism for disseminating the results of its research and development activities. These results are published by NASA in the NASA STI Report Series, which includes the following report types:

- TECHNICAL PUBLICATION. Reports of completed research or a major significant phase of research that present the results of NASA programs and include extensive data or theoretical analysis. Includes compilations of significant scientific and technical data and information deemed to be of continuing reference value. NASA counterpart of peer-reviewed formal professional papers, but having less stringent limitations on manuscript length and extent of graphic presentations.

- TECHNICAL MEMORANDUM. Scientific and technical findings that are preliminary or of specialized interest, e.g., quick release reports, working papers, and bibliographies that contain minimal annotation. Does not contain extensive analysis.

- CONTRACTOR REPORT. Scientific and technical findings by NASA-sponsored contractors and grantees.

- CONFERENCE PUBLICATION. Collected papers from scientific and technical conferences, symposia, seminars, or other meetings sponsored or co-sponsored by NASA.

- SPECIAL PUBLICATION. Scientific, technical, or historical information from NASA programs, projects, and missions, often concerned with subjects having substantial public interest.

- TECHNICAL TRANSLATION. English-language translations of foreign scientific and technical material pertinent to NASA's mission.

Specialized services that complement the STI Program Office's diverse offerings include creating custom thesauri, building customized databases, organizing and publishing research results ... even providing videos.

For more information about the NASA STI Program Office, see the following:

- Access the NASA STI Program Home Page at ***http://www.sti.nasa.gov***

- E-mail your question via the Internet to help@sti.nasa.gov

- Fax your question to the NASA STI Help Desk at (301) 621-0134

- Phone the NASA STI Help Desk at (301) 621-0390

- Write to:
  NASA STI Help Desk
  NASA Center for AeroSpace Information
  7121 Standard Drive
  Hanover, MD 21076-1320

NASA/TM-2001-211243

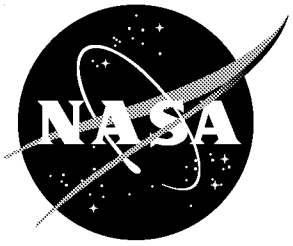

System Identification and Pod Method Applied to Unsteady Aerodynamics

Deman Tang and Denis Kholodar
Duke University, Durham, North Carolina

Jer-Nan Juang
Langley Research Center, Hampton, Virginia

Earl H. Dowell
Duke University, Durham, North Carolina

National Aeronautics and
Space Administration

Langley Research Center
Hampton, Virginia 23681-2199

December 2001

Available from:

NASA Center for AeroSpace Information (CASI)
7121 Standard Drive
Hanover, MD 21076-1320
(301) 621-0390

National Technical Information Service (NTIS)
5285 Port Royal Road
Springfield, VA 22161-2171
(703) 605-6000

SYSTEM IDENTIFICATION AND POD METHOD APPLIED TO UNSTEADY AERODYNAMICS

Deman Tang * and Denis Kholodar †
Duke University, Durham, North Carolina 27708-0300
Jer-Nan Juang ‡
NASA Langley Research Center, Hampton, VA 23681
Earl H. Dowell §
Duke University, Durham, North Carolina 27708-0300

ABSTRACT

The representation of unsteady aerodynamic flow fields in terms of global aerodynamic modes has proven to be a useful method for reducing the size of the aerodynamic model over those representations that use local variables at discrete grid points in the flow field. Eigenmodes and Proper Orthogonal Decomposition (POD) modes have been used for this purpose with good effect. This suggests that system identification models may also be used to represent the aerodynamic flow field. Implicit in the use of a systems identification technique is the notion that a relative small state space model can be useful in describing a dynamical system. The POD model is first used to show that indeed a reduced order model can be obtained from a much larger numerical aerodynamical model [the vortex lattice method is used for illustrative purposes] and the results from the POD and the system identification methods are

*Research Associate Professor, Dept. of Mechanical Engineering and Materials Science. Member AIAA
†Research Assistant, Dept. of Mechanical Engineering and Materials Science.
‡Principal Scientist, Structural Dynamics Branch. Fellow AIAA
§J. A. Jones Professor, Dept. of Mechanical Engineering and Materials Science. Fellow AIAA

then compared. For the example considered, the two methods are shown to give comparable results in terms of accuracy and reduced model size. The advantages and limitations of each approach are briefly discussed. Both appear promising and complementary in their characteristics.

INTRODUCTION

In recent work it has been shown that the use of a modal representation of unsteady aerodynamic flow fields has many advantages [1-4]. Among these is the ability to reduce the order of a computational fluid dynamics (CFD) code from many thousands of degrees of freedom to several tens of degrees of freedom while retaining essentially the same accuracy of representation of fluid forces acting on a wing. Recognizing that the aerodynamic forces may be expressed in terms of aerodynamic modes, this suggests that in some cases it may be advantageous to use a system identification method to determine a modal representation of the aerodynamic forces. For example, this could be done using either numerical data from a CFD code or experimental data from a wind tunnel test. Here we explore this possibility and compare the results obtained from a system identification procedure and those obtained by a direct determination of the aerodynamic modes from a theoretical fluid dynamics model. In the present study, a three-dimensional time domain vortex lattice aerodynamic model and the Proper Orthogonal Decomposition(POD) method are used to investigate the unsteady flow about an oscillating delta wing. The POD modes and the eigenmodes of the vortex lattice model are determined starting from a time history of the flow field computed for a step change in angle of attack (or plunge velocity). This same set of time histories is then provided as the input data for a system identification technique as discussed in [5] to determine a dynamic model of the aerodynamic system. The eigenvalues of this identified system are then compared to those determined using the POD method and the vortex lattice model. Excellent agreement is found between the two results, thus confirming the ability of system identification methods to extract useful information from numerically determined time histories based upon a theoretical computational model. This also suggests that a similar procedure might be successful that employs numerical data from more complex CFD models or from measured experimental data. In the following sections, discussed in order

are the Aerodynamic Model, the Proper Orthogonal Decomposition Method, the System Identification Method and an Example using numerical data from a simulated time history.

AERODYNAMIC MODEL

The flow about a cantilevered half-span delta wing is assumed to be incompressible, inviscid and irrotational. Here an unsteady vortex lattice method is used to model this flow. Kim [4] has also used a similar flow model in his study of the POD or Karhunen-Loeve method for a wing of rectangular planform. A typical planar vortex lattice mesh for the three-dimensional flow over a delta wing is shown in Figure 1. The plate and wake are divided into a number of elements. In the wake and on the wing all the elements are of equal size, Δx, in the streamwise direction. For the present calculations, the spanwise element size, Δy, is chosen to be equal to Δx. Point vortices are placed on the plate and in the wake at the quarter chord of the elements. At the three-quarter chord of each plate element a collocation point is placed for the downwash, the velocity induced by the discrete vortices is set equal to the downwash arising from the step angle of attack of the delta wing. Thus one has the relationship,

$$w_i^{t+1} = \sum_j^{kmm} K_{ij}\Gamma_j^{t+1}, \qquad i = 1, ...km \tag{A1}$$

where w_i^{t+1} is the downwash at the ith collocation point at time step $t+1$, Γ_j is the strength of the jth vortex. Γ is normalized by cU and w by U where U is the freestream velocity. K_{ij} is an aerodynamic kernel function. An aerodynamic matrix equation to determine Γ can be expressed as,

$$[A]\{\Gamma\}^{t+1} + [B]\{\Gamma\}^t = [T]\{w\}^{t+1} \tag{A2}$$

where $[A]$ and $[B]$ are aerodynamic coefficient matrices and $[T]$ is a transfer matrix for determining the relationship between the global vortex lattice mesh and the local vortex lattice mesh on the delta wing itself. Expressions for A, B and T are given in Ref.[1].

From the fundamental aerodynamic theory, the pressure distribution on the wing can be obtained at the jth point in terms of the vortex strengths. The pressure difference between

the wing plate upper and lower surfaces at $x = x_j, y = y_j$ is given by

$$\Delta p^{t+1}(x_j, y_j) = \rho U^2 \frac{c}{\Delta x}[(\Gamma^{t+1}(x_j, y_j) + \sum_{i=1}^{j}(\Gamma^{t+1}(x_i, y_j) - \Gamma^{t}(x_i, y_j))] \tag{A3}$$

The local total lift at $y = y_j$ is obtained by integrating the pressure difference along the local chord-line.

$$L_{local}^{t+1}(y_j) = \int_0^{c_{local}} \Delta p^{t+1}(x, y_j)dx$$

where $c_{local} = cy_j/l$ and l is span length and c is the root chord. The total lift is obtained by integrating the local total lift along the span.

$$L^{t+1} = \int_0^l L_{local}^{t+1}(y)dy = c\sum_{j=1}^{k_n} L_{local}^{t+1}(y_j)\Delta\overline{y}$$

where $\Delta\overline{y} = 1/k_n$ and k_n is the number of spanwise discrete elements. The total aerodynamic lift coefficient, C_L is defined by

$$C_L^{t+1} = L^{t+1}/\tfrac{1}{2}\rho U^2 A_w \tag{A4}$$

where A_w is the total wing area. In the present example, $A_w = \frac{1}{2}c^2$ and $\Delta\overline{y} = \frac{1}{15}$

The numerical model is a simple delta wing configuration with a leading edge sweep of 45 degrees. We use an aerodynamic vortex lattice model with 120 vortex elements on the delta wing (km=kn=15) and 525 vortex elements in the wake (kmm=50). The total number of vortex elements is N=645.

SINGULAR VALUE DECOMPOSITION, PROPER ORTHOGONAL DECOMPOSITION AND BALANCED MODES: A GENERIC DISCUSSION

Let $q(j)$ be the nth flow variable at some spatial point at some time j where $n = 1, ..., N$ and $j = 1, ..., J$. Now form the matrix, $\hat{Q}$, as

$$\left[\hat{Q}\right]_{N\times J} = \begin{bmatrix} q^1(1) & ..... & q^1(J) \\ : & : & : \\ q^N(1) & ..... & q^N(J) \end{bmatrix} \tag{1}$$

Again note the total number of time steps is J and the total number of flow variables is N. For a typical CFD calculation, J might be 1000 and N might be 10000 or more. Hence N is much greater than J.

Now assume a singular value decomposition of $\hat{Q}$ i.e.

$$[\hat{Q}] = [U][\Sigma][V]^T \tag{2}$$

where U is a unitary matrix of dimension $N \times n$ and V is also a unitary matrix of dimension $J \times n$. One may select n and typically n will be less than J. Note that

$$[U]^T[U] = [I]_{n\times n} \qquad , \qquad [V]^T[V] = [I]_{n\times n} \tag{3}$$

and Σ is a diagonal matrix of singular values, i.e.

$$[\Sigma]_{n\times n} = \begin{bmatrix} \sigma_1 & & & & \\ & \sigma_2 & & & \\ & & . & & \\ & & & . & \\ & & & & \sigma_n \end{bmatrix} \tag{4}$$

Now order these singular values such that

$$\sigma_1 \geq \sigma_2 \geq .....\sigma_n \tag{5}$$

Form Φ, the correlation matrix for the POD method.

$$[\Phi] \equiv [\hat{Q}]^T[\hat{Q}] = [V][\Sigma]^T[U]^T[U][\Sigma][V]^T = [V][\Sigma]^T[\Sigma][V]^T \tag{6}$$

Equation (6) implies that V is the eigenvector of the correlation matrix and the corresponding eigenvalues are the squares of the singular values. From Equation (2), one may compute (assuming that V is normalized so that the magnitude of each eigenvector is unity)

$$[\hat{Q}][V] = [U][\Sigma][V]^T[V] = [U][\Sigma] \tag{7}$$

One may also compute U from Equation (7) and further one may compute $\hat{Q}$ from a knowledge of U, V and the singular values using Equation (2). Usually it is easier to compute

$\hat{Q}$ directly from Equation (1). However the representation of Equation (2) may be useful if one chooses to decompose $\hat{Q}$ such that

$$[\hat{Q}] = ([U][\Sigma]^{1/2})([\Sigma]^{1/2}[V]^T) \tag{8}$$

With this decomposition the POD modes are said to be "balanced" and these are often put forth as an optimum choice for mode selection.

If there is a truncation in the singular values, i.e. one chooses n to be less than J which is much less than N, then Equation (2) may be written in a reduced form. The corresponding reduced form for $\hat{Q}$ approaches the original $\hat{Q}$ if the neglected singular values or POD eigenvalues are sufficiently small compared to those retained.

Denoting V as the eigenvector matrix for the correlation matrix of dimension $J \times n$, noting that $\hat{Q}$ is a matrix of $N \times J$, and defining, a, as the new unknowns to be determined which are the n modal amplitudes of the POD modes, then one may write the original flow variables, q, as

$$\{q^{(t)}\}_{N\times 1} = [\hat{Q}]_{N\times J}[V]_{J\times n}\{a\}_{n\times 1} \tag{9}$$

Substituting this expression into a generic form of the flow equations of motion, i.e.

$$\{\frac{dq}{dt}\} = \{Q(q)\} + \{B\}u \tag{10}$$

and pre-multiplying by the transpose of $\hat{Q}$ gives a reduced order model in terms of the new unknowns, a ,where the dimension of the vector a is $n \times 1$ with n chosen to be less than J.

For simplicity, in Equation (10) only a single scalar input, u, is shown. The generalization to multiple inputs is clear. If $Q(q)$ in Equation (10) is expanded in a Taylor Series about a steady flow solution (the time linearized model corresponds to retaining only linear terms in q in the Taylor Series), then a particularly simple and attractive form of the reduced order model is obtained.

There is another interesting case to consider which may arise when experimental data rather than numerical data from a CFD code are used to construct a reduced order model. In this case the number of flow variables that are observed or measured, N, will be relatively small and typically N will be less than J, the total number of time steps for which data are

obtained. Formally the calculation still goes through, but now the number of flow variables modeled is much smaller than for a CFD code. Ideally these flow variables would be related to the amplitudes of the dominant modes of the flow.

SYSTEM IDENTIFICATION

To conform to the usual formalism of system identification theory, we consider a discrete time state space model [4]. Note the vortex lattice flow model naturally appears in this form. For continuous time models, the relationship between discrete and continuous time representations must be carefully considered. Formally the procedure is similar, however.

Assume that the flow field can be described by the discrete-time state-space model,

$$x(k+1) = Ax(k) + Bu(k) \tag{11}$$

$$y(k) = Cx(k) + Du(k)$$

where $x(k)$ is a state vector of $n \times 1$ (n=order of the system), $u(k)$ is an input force vector of $\gamma \times 1$ (γ=number of input), $y(k)$ is an output measurement vector of f $m \times 1$ (m=number of output). The matrices A, B, C, and D, are the state matrix, input matrix, output matrix, and direct transmission matrix, respectively.

Let $u_i(0) = 1(i = 1, 2, ...\gamma)$ and $u_i(k) = 0(k = 1, 2, ...)$ be substituted into Eq.(11). When the substitution is performed for each input element $u_i(0) = 1(i = 1, 2, ...\gamma)$, the results can be assembled into a pulse response matrix Y with dimension m by r as follows:

$$Y_0 = D, Y_1 = CB, Y_2 = CAB, ..., Y_k = CA^{k-1}B \tag{12}$$

The constant matrices in the sequence are known as Markov parameters (See [4]).

Assume that the scalar quantity $q_i(k)$ in the matrix Q in Eq.(1) is the pulse response of the ith flow variable at the time step k corresponding to a pulse input. A column vector Y

can be formed by

$$Y_1 = CB = \begin{bmatrix} q_1(1) \\ q_2(1) \\ : \\ : \\ q_m(1) \end{bmatrix}, Y_2 = CAB = \begin{bmatrix} q_1(2) \\ q_2(2) \\ : \\ : \\ q_m(2) \end{bmatrix}, ...Y_k = CA^{k-1}B = \begin{bmatrix} q_1(k) \\ q_2(k) \\ : \\ : \\ q_m(k) \end{bmatrix} \tag{13}$$

System identification begins by forming the generalized Hankel matrix $H(0)$, composed of the Markov parameters

$$H(0) = \begin{bmatrix} Y_1 & Y_2 & .... & Y_{l-1} \end{bmatrix} \tag{14}$$

This matrix is identical to the matrix Q in Eq.(1) with the absence of the last column. Here as assumption has been made, i.e., $m > l > n$. For the other cases where the number of measurement sensors is sufficiently less than the order of the system, i.e., $l > n > m$, a different Hankel matrix can be formed for system identification (see Chapter 5 in [4]). The fundamental rule is that the Hankel matrix must be formed such that its rank is larger than the order of the system to be identified.

In theory, the Hankel matrix $H(0)$ and the state-space model are related by

$$\begin{aligned} H(0) &= \begin{bmatrix} Y_1 & Y_2 & .... & Y_{l-1} \end{bmatrix} \\ &= \begin{bmatrix} CB & CAB & .... & CA^{l-2}B \end{bmatrix} \\ &= C \begin{bmatrix} B & AB & .... & A^{l-2}B \end{bmatrix} \end{aligned} \tag{15}$$

To determine A, B, C, first decompose the matrix $H(0)$ by using singular value decomposition to yield

$$\begin{aligned} H(0) &= U\Sigma V^T = [U_r \ \mathrm{U}_t] \begin{bmatrix} \Sigma_r & O_{n-r} \\ O_{n-r} & \Sigma_t \end{bmatrix} [V_r \ \mathrm{V}_t]^T \\ &= U_r\Sigma_r V_r^T + U_t\Sigma_t V_t^T \\ &\approx U_r\Sigma_r V_r^T \\ &= [U_r\Sigma_r^{1/2}][\Sigma_r^{1/2}V_r] \end{aligned} \tag{16}$$

Comparison of Eqs.(15) and (16) established the following equalities

$$[U_r\Sigma_r^{1/2}] = C$$

$$[\Sigma_r^{1/2} V_r] = \left[\begin{array}{cccc} B & A & .... & A^{l-2} \end{array} \right] \tag{17}$$

The equalities are not unique, but they are balanced because both share the matrix Σ equally. The matrix B is then determined by

$$B = \text{ The first column of } [\Sigma_r^{1/2} V_r] \tag{18}$$

To determine the state matrix A, another Hankel matrix must be formed, i.e.,

$$H(1) = \left[\begin{array}{cccc} Y_2 & Y_3 & .... & Y_l \end{array} \right] \tag{19}$$

This matrix is formed by deleting the first column of $H(0)$ and adding a new column at the end of the matrix. As a result, $H(1)$ has the following relationship with the system matrices A, B, and C

$$\begin{aligned} H(1) &= \left[\begin{array}{cccc} Y_2 & Y_3 & .... & Y_l \end{array} \right] \\ &= \left[\begin{array}{cccc} CAB & CA^2B & .... & CA^{l-1}B \end{array} \right] \\ &= CA \left[\begin{array}{cccc} B & AB & .... & A^{l-2}B \end{array} \right] \end{aligned} \tag{20}$$

Substituting Eq.(17) into Eq.(20) thus yields

$$\begin{aligned} A &= [U_r \Sigma_r^{1/2}]^{\dagger} H(1) [\Sigma_r^{1/2} V_r]^{\dagger} \\ &= \Sigma_r^{-1/2} U_r^T H(1) V_r^T \Sigma_r^{-1/2} \end{aligned} \tag{21}$$

The symbol $\dagger$ means pseudo-inverse. The orthonormal property of U and V shown in Eq.(3) has been used to derive Eq.(21).

Assume that the state matrix A of order r has a complete set of linearly independent eigenvectors $\psi_1, \psi_2, ..., \psi_r$ with corresponding eigenvalues $\lambda_1, \lambda_2, ..., \lambda_r$ which are not necessarily distinct. Define Λ as the diagonal matrix of eigenvalues and Ψ as the matrix of eigenvectors, i.e.,

$$\Lambda = \left[\begin{array}{cccc} \lambda_1 & & & \\ & \lambda_2 & & \\ & & . & \\ & & & \\ & & & \lambda_r \end{array} \right] \tag{22}$$

and

$$\Psi = \left[\begin{array}{cccc} \psi_1 & \psi_2 & \ldots & \psi_r \end{array} \right] \tag{23}$$

The identified A, B, and C can then be transformed to become $\Lambda, \Psi^{-1}B$, and $C\Psi$. The diagonal matrix Λ contains the information of modal damping rates and damped natural frequencies. The matrix $\Psi^{-1}B$ defines the initial modal amplitudes and the matrix $C\Psi$ the mode shape at the sensor points. All the modal parameters of a dynamic system can thus be identified by the three matrices $\Lambda, \Psi^{-1}B$, and $C\Psi$. The desired modal damping rates and damped natural frequencies are simply the real and imaginary parts of the eigenvalues Λ_c, after transformation from the discrete-time domain to the continuous-time domain using the relation

$$\Lambda_c = \frac{1}{\Delta t} Log(\Lambda) \tag{24}$$

AN EXAMPLE

1. POD model:

In this example $J = 100$ time steps and Equation (A2) is marched in time to determine Γ for a unit step change in angle of attack. Identifying Γ with the flow variables, q, we form $\hat{Q}$ and Φ. See Equations (1) and (6). From Eq.(6), one obtains the POD eigenvector V and the corresponding POD eigenvalues of $\Sigma^T\Sigma$. We normalize the POD eigenvectors V such that

$$[V]^T[V] = [I]$$

The POD eigenvalues calculated are shown in Table 1. Examining these 100 eigenvalues, one finds the first few modes are the most important. Also found are some very small negative eigenvalues because of the numerical roundoff error in the eigenvalue calculation. Note that the POD eigenvalues and eigenvectors are <u>not</u> the eigenvalues and eigenvectors of Γ per se. The latter maybe determined from Eq.(A2) or approximately from the reduced order model.

From Eq.(2), we can determine the unitary matrix U,

$$[U] = [\hat{Q}][V][\Sigma]^{-1} \tag{25}$$

with a normalization such that $[U]^T[U] = [I]$. From Eq.(A2), we have

$$\{\Gamma\}^{t+1} + [A]^{-1}[B]\{\Gamma\}^t = [A]^{-1}[T]\{w\}^{t+1} \tag{26}$$

From Eq.(9), We have

$$\{\Gamma\} = [\hat{Q}]_{N\times J}[V]_{J\times n}\{a\}_n$$

Substituting Eq.(25) into Eq.(9), we have

$$\{\Gamma\} = [U][\Sigma]\{a\} \tag{27}$$

Substituting Eq.(27) into Eq.(26), we have

$$[U][\Sigma]\{a\}^{t+1} + [A]^{-1}[B][U][\Sigma]\{a\}^t = [A]^{-1}[T]\{w\}^{t+1} \tag{28}$$

Pre-multiplying by the transpose of $[U][\Sigma]$ gives a reduced order model in terms of the new unknowns, $\{a\}$.

$$([U][\Sigma])^T[U][\Sigma]\{a\}^{t+1} + ([U][\Sigma])^T[A]^{-1}[B][U][\Sigma]\{a\}^t = ([U][\Sigma])^T[A]^{-1}[T]\{w\}^{t+1} \tag{29}$$

Thus a new three-dimensional time domain vortex lattice aerodynamic equation is given by

$$\{a\}^{t+1}_{n\times 1} + [P]_{n\times n}\{a\}^t_{n\times 1} = [R]_{n\times N}\{w\}^{t+1}_{N\times 1} \tag{30}$$

where

$$[P] = ([\Sigma]^T[\Sigma])^{-1}([U][\Sigma])^T[A]^{-1}[B][U][\Sigma]$$

and

$$[R] = ([\Sigma]^T[\Sigma])^{-1}([U][\Sigma])^T[A]^{-1}[T]$$

Generally, $n << N$, and thus a reduced order time domain equation is obtained. For the present example, $N = 645$ and $n \leq 20$. Once $\{a\}$ is determined from Eq.(30), the $\{\Gamma\}^t$ and $\{\Gamma\}^{t+1}$ can be determined from Equation (26) and the total lift coefficient of the delta wing is calculated using Eq.(A4).

Figure 2 shows the total lift coefficient of the delta wing vs nondimensional time, τ, as determined from the full vortex lattice model i.e , using Eq.(A2) with $N = 645$.

Figure 3 shows the total lift coefficient of the delta wing vs nondimensional time, τ, as determined from the reduced order model for various sizes of the reduced order model, i.e. $n = 1, 5$ and $n = 20$, using Eq.(30).

The reduced order model results are very close to the result using the full vortex lattice model for the steady state, $\tau \to \infty$ even for $n = 1$. These results are consistent with those of Table 1. As seen from this table, the POD eigenvalue of the first mode is significantly larger than the others. So there is a single dominant mode and all others have a relatively small contribution to the total lift coefficient. However more POD modes are required to capture the dynamics of the flow model for shorter times, say $\tau < 1$, as shown in Figure 3.

The aerodynamic eigenvalues of the vortex lattice model may be determined from Eq.(26) and an approximation to these eigenvalues may be determined from Eq.(30) by setting the right hand sides to zero and determining the condition for non-trivial solutions in the usual way. Results from these calculations will be compared to those obtained from the system identification method in the following discussion.

2. System identification:

Using the time history for the vortex strengths of the vortex lattice model at each grid point, the system identification procedure described earlier was used to construct a dynamical model of this system. By using all the information of the original model we can be sure that we will reproduce these same time histories to some specified accuracy and that is indeed the case. Within plotting error, the results for the time history of the original vortex lattice model and that of the identified model are identical.

More interesting is the number of states required in the system identification model to achieve this accuracy and how well the eigenvalues of the identified model agree with those of the original model. It turns out that the number of states in the identified model is about 40, i.e. of the same order as the number of states required in the POD model to reproduce

the essential dynamics of the original vortex lattice model.

It has been shown in previous work that the dominant eigenvalues of the vortex lattice model may be represented by the POD modes. In Figure 4 we show a comparison between the eigenvalues determined from the full vortex model and those determined from the system identification model. As is seen the agreement between the two results is excellent for the corresponding eigenvalues. The identified model in fact has represented the eigenmodes in the dominant branch of the eigenvalue distribution of the original vortex lattice model and done so with a high degree of accuracy.

The dominant branch of the eigenvalue distribution corresponds to the eigenmodes with a spanwise pressure distribution similar to that for the lift on a wing at steady angle of attack. Other branches of the eigenvalue distribution correspond to higher spanwise modal forms.

A system identification (SID) model for an unsteady aerodynamic flow has been created for several wing motions or gust excitations and corresponding aerodynamic responses. These models were derived from numerical simulations using a vortex lattice (VL) model for the delta wing with 55 vortex elements on the wing and 300 vortex elements in the wake (e.g. km=kn=10, kmm=40 as shown in Fig. 1). In each case, the flow about the wing is excited by a certain type of prescribed downwash at the wing grid points, $w(t)$. The numerical VL model produced vortex strengths at the grid points of the wing and in the wake, $\Gamma(t)$, and the corresponding pressure distribution on the wing, $p(t)$. These data were then used as input for the SID code.

The excitations to the flow that have been considered are

1) step angle of attack, $w(t) = const$ for $t > 0$,

2) sharp edge gust, $w(t - x/u) = const$ for $(t - x/u) > 0$,

3) frozen gust of changing frequency,

$$w(t - x/u) = const \times \sin(\omega(t - x/u)^2/2T)$$

such a gust is sometimes called a swept gust, and finally

4) random downwash (w at each grid point and at every time step is a random number).

First, the SID model was used to reproduce the time histories of the vortex strength (on the wing and in the wake) for 100 time steps. Results obtained from the SID model were almost identical to those of the original VL model. The plots of such time histories are not provided here, because one would not be able to see the difference in the time series of the original data and the time series obtained via SID. However, to quantify the differences between VL and SID outputs an error, δ, defined as $\delta = 100\%|Q - y|/|Q|$ was used, where the norm $|X|$ is defined to be the largest singular value of X. In this case, both Q (VL) and y (SID) are 100×355 rectangular matrices (100 time steps and 355 degrees of freedom). For the above mentioned aerodynamic problems, and given the vortex strengths everywhere, the error was less than 0.05%. Moreover, using the VL time series for the vortex strengths only on the wing, the SID model reproduced them with almost the same accuracy – the largest (among the aforementioned cases) error was 0.1%. The number of singular values retained in the identified model varied from 60 to 90 for the cases when vortex strengths were provided only on the wing and from 60 to 160 for the cases when the SID used vortex strengths both on the wing and in the wake. (The number of singular values kept was such that the ratio of the largest singular value to the smallest one kept was 10^{-12}.)

Next the ability of such a SID model to capture the eigenmodes of the original VL system and especially the dominant eigenmodes was studied. Here again, all the information on the wing and wake was used initially, and then the information only on the wing was used to obtain the eigenvalues. The former case is shown in Figures 5 and 6 and the latter in Figure 7. Here the original VL eigenvalues are shown as circles and the eigenvalues obtained from the SID model are indicated by crosses. In the case of full information, the dominant eigenvalue branch for the case of a step angle of attack (Fig. 5a) and also a sharp edge gust (Fig. 5b) is captured nicely (36 singular values and 57 singular values were used respectively in the SID model). For the case of a swept gust (Fig. 5c) and random downwash (Fig. 5d), the SID model produced sets of eigenvalues that do not agree well with the original ones from the VL code (164 singular values and 99 singular values were used respectively in the SID model). However, for the problem of the random downwash, increasing the length of the time history that was used as input to the SID model code from 100 steps to 1000 steps lead to a set of eigenvalues that is in very good agreement with the dominant branch as shown

in Figure 6 (250 singular values were used).

When the vortex strengths only on the wing were used for some initial selection of parameters in the SID model (see Fig. 7), interestingly the dominant branch of eigenvalues is recovered not only for the step angle of attack (Fig. 7a) and the sharp edge gust (Fig. 7b), but also for the case of the swept gust (Fig. 7c) and random downwash (Fig. 7d), even though in the last case the dominant branch identified by the SID model is somewhat "off target". By looking at the Figure 7 one might conclude that providing vortex strength information only on the wing in these cases is sufficient for finding the distinct dominant eigenvalue branch. However, one should not conclude that using vortex strength information on the wing only is actually better than using information about vortex strengths both on the wing and in the wake.

By running the SID code for various parameter choices and for a certain number of retained singular values, different lengths of time series, using information on the wing only vs information everywhere, etc, the authors have found, firstly, that the set of eigenvalues from the SID model could either include the "correct" dominant eigenvalue branch or could be a different set of eignvalues (which, by the way, does not prevent the SID model from reproducing the original time series with excellent agreement); secondly, it was concluded that if there is a distinct branch of eigenvalues found from the SID model, it is most likely to be similar to the dominant branch in the original VL model.

Now another case will be considered. In the context of wing tunnel or flight experiments, one is also interested in what can be identified from the measured data such as pressure. So using numerically obtained pressure values over the wing, the SID model was used to reproduce pressure time histories. Just as in the case of vortex strength data on the wing only, 55 pressure time histories of 100 time steps were input to the SID code. Using 30 to 40 singular values, the error between the original and identified time histories of pressure remained less than 1%.

One could argue that it may be impractical to use such a large amount of sensors on the wing to apply SID models. Thus, next only a portion of the pressure data on the wing was used. Different sensor positions were considered. A discussion of the various downwash and sensor locations on such a wing is ommitted here. For the current discussion, leading edge

elements from the root to the tip of the wing were taken, as they appear to be a very good choice for system identification purposes. In Figure 8, results for the pressure time history at the tip element of the wing are shown for the case when 10 measurements (still numerically simulated, of course) of the downwash and pressure time history (100 time steps) along the leading edge were supplied to create the SID model. Using from 50 to 90 singular values for the four aerodynamic loading problems, the previously defined error ranged from 0.002% to 1.8%.

However, using pressure data only, no success has yet been realized in approximating the eigenvalues of the original VL model. This is a subject of continuing investigation.

CONCLUDING REMARKS

It has been shown that a modal representation of the aerodynamic forces acting on an oscillating wing has several attractive features that may be exploited. As has been shown earlier, starting from a numerical model of the fluid, here taken to be a vortex lattice model, the fluid model may be efficiently represented in terms of Proper Orthogonal Decomposition (POD) modes. However it was also shown that using standard system identification techniques for linear dynamical systems, an identified system model may also be constructed using data from the numerical model. Both the POD modes and the system identification method lead to substantially reduced order models of the flow field of comparable dimensions. And therefore both provide highly efficient computational models relative to the original [vortex lattice] numerical model.

In principle the POD method may also be used for nonlinear dynamical systems. However much work has yet to be done to implement this capability in the context of unsteady aerodynamic models. The system identification methodology for nonlinear dynamical systems is still a research frontier and no general methods are yet available. On the other hand the systems identification approach may be useful when only partial flow field data are available, e.g. from a wind tunnel experiment, and this aspect is currently under investigation by the authors.

Finally it is noted that although a particular numerical model of the fluid was used in the

present paper, i.e. a vortex lattice model, no especial difficulty is expected in extending these methods to other Computational Fluid Dynamics (CFD) models. Indeed the beneficial use of POD for a variety of CFD models has been shown in [1-3]. Since the system identification model only requires time histories or Fourier Series (frequency domain) data from such a CFD model, the extension to any time linearized CFD model is straightforward. Indeed even if the original CFD model is not time linearized per se, the code can be run for small wing motions to simulate numerically time linearized conditions.

ACKNOWLEDGMENTS

This work was supported under AFOSR Grant, "Limit Cycle Oscillations and Nonlinear Aeroelastic Wing Response". Dr. Daniel Segalman is the grant program officer. All numerical calculations were done on a supercomputer, T916, in the North Carolina Supercomputing Center (NCSC).

REFERENCES

1. Hall, K.C., " Eigenanalysis of Unsteady Flows About Airfoils, Cascades, and Wings," *AIAA Journal*, Vol.32, No.12, 1994, pp. 2426-2432.

2. Dowell, E.H., Hall, K.C., and Romanowski, M.C., " Eigenmode Analysis in Unsteady Aerodynamics: Reduced Order Models," *Applied Mechanics Reviews*, Vol.50, No.6, June 1997, pp. 371-385.

3. Dowell, E.H. and Hall, K.C., " Modeling of Fluid-Structure Interaction," Invited Chapter in the *Annual Reviews of Fluid mechanics*, Vol. 33, 2001, pp. 445-490.

4. Kim, T., "Frequency-Domain Karhunen-Loeve Method and Its Application to Linear Dynamic System," *AIAA Journal*, Vol. 36, No.11, November 1999, pp.2117-2123.

5. Juang, J.-N., *Applied System Identification*, Prentice Hall, Inc., Englewood Cliffs, New Jersey 07632, 1994, ISBN 0-13-079211-X.

Table 1: Eigenvalues, σ_n

σ_{1-25}	σ_{26-50}	σ_{51-75}	σ_{76-100}
0.31168E+03	0.51654E+00	0.82697E-05	-0.33688E-05
0.33737E+02	0.50582E+00	-0.80430E-05	-0.30680E-05
0.39184E+01	0.49650E+00	-0.77611E-05	-0.26678E-05
0.31482E+01	0.48854E+00	-0.72553E-05	-0.27129E-05
0.25025E+01	0.48179E+00	0.75330E-05	-0.22659E-05
0.20812E+01	0.47621E+00	0.72555E-05	-0.16534E-05
0.17607E+01	0.47171E+00	-0.69035E-05	0.32531E-05
0.15281E+01	0.46827E+00	-0.65890E-05	0.29655E-05
0.13464E+01	0.46584E+00	-0.62088E-05	0.28340E-05
0.12051E+01	0.46439E+00	-0.64251E-05	0.25623E-05
0.10909E+01	0.15028E+00	-0.57141E-05	0.24380E-05
0.99799E+00	0.85771E-02	0.65583E-05	-0.13306E-05
0.92088E+00	0.84648E-04	0.64960E-05	-0.11599E-05
0.85612E+00	-0.17071E-04	0.60496E-05	-0.84823E-05
0.80130E+00	0.13413E-04	0.57069E-05	-0.46961E-05
0.75427E+00	0.12234E-04	-0.52226E-05	-0.34102E-06
0.71385E+00	-0.10651E-04	-0.48201E-05	-0.12280E-06
0.67867E+00	-0.10369E-04	-0.42629E-05	0.18361E-05
0.64813E+00	0.11271E-04	0.49989E-05	0.17704E-05
0.62129E+00	0.10661E-04	0.47778E-05	0.14315E-05
0.59783E+00	-0.90705E-05	0.47381E-05	0.12146E-05
0.57712E+00	0.99622E-05	0.43455E-05	0.10583E-05
0.55896E+00	0.96568E-05	0.39997E-05	0.44381E-06
0.54293E+00	0.90764E-05	-0.37350E-05	0.49844E-06
0.52889E+00	-0.85099E-05	-0.35918E-05	0.60061E-06

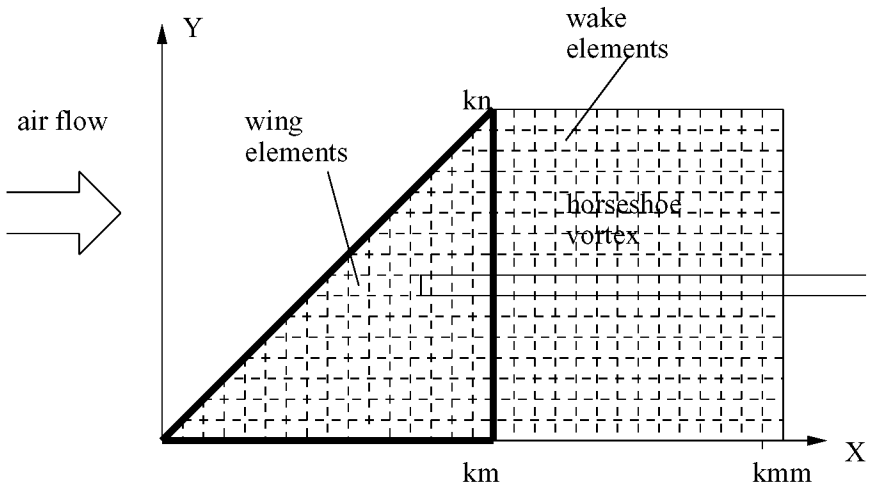

Figure 1: Numerical grid for delta wing-plate using vortex lattice aerodynamic model

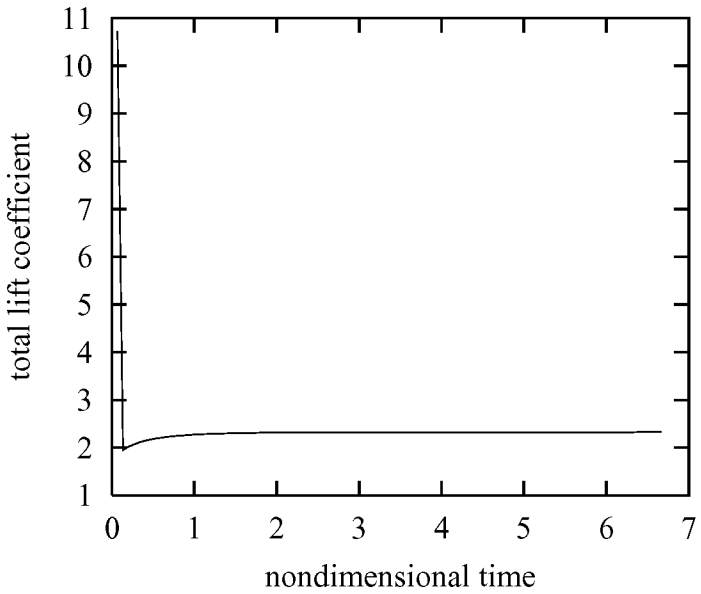

Figure 2: The total lift coefficient of the delta wing vs nondimensional time, τ, for all modes

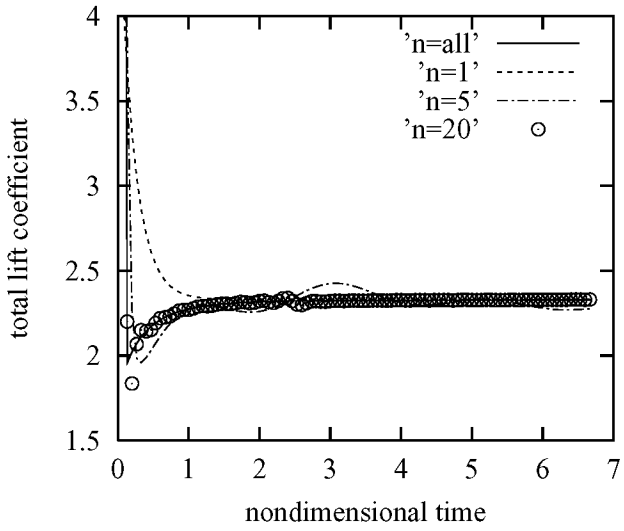

Figure 3: The total lift coefficient of the delta wing vs nondimensional time, τ, for $n = 1, 5$ and $n = 20$

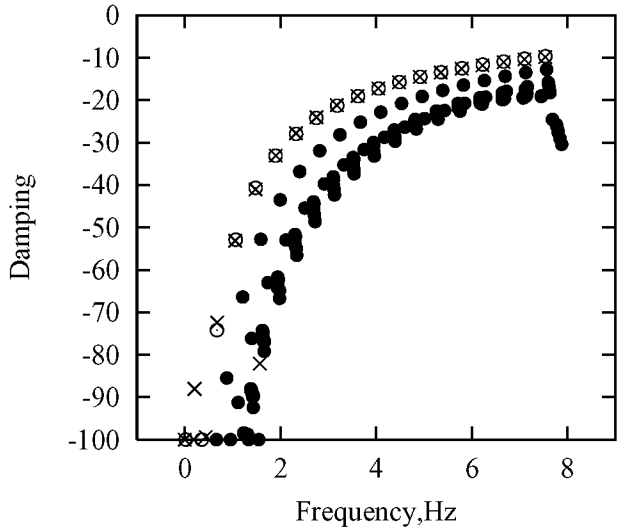

Figure 4: Eigenvalue solutions of vortex lattice model of unsteady three-dimensional flow about a delta wing. Eigenvalues determined directly from the vortex lattice model: $\circ$ Dominant branch of eigenvalues, $\bullet$ All other eigenvalues; Eigenvalues from system identification model: $\times$.

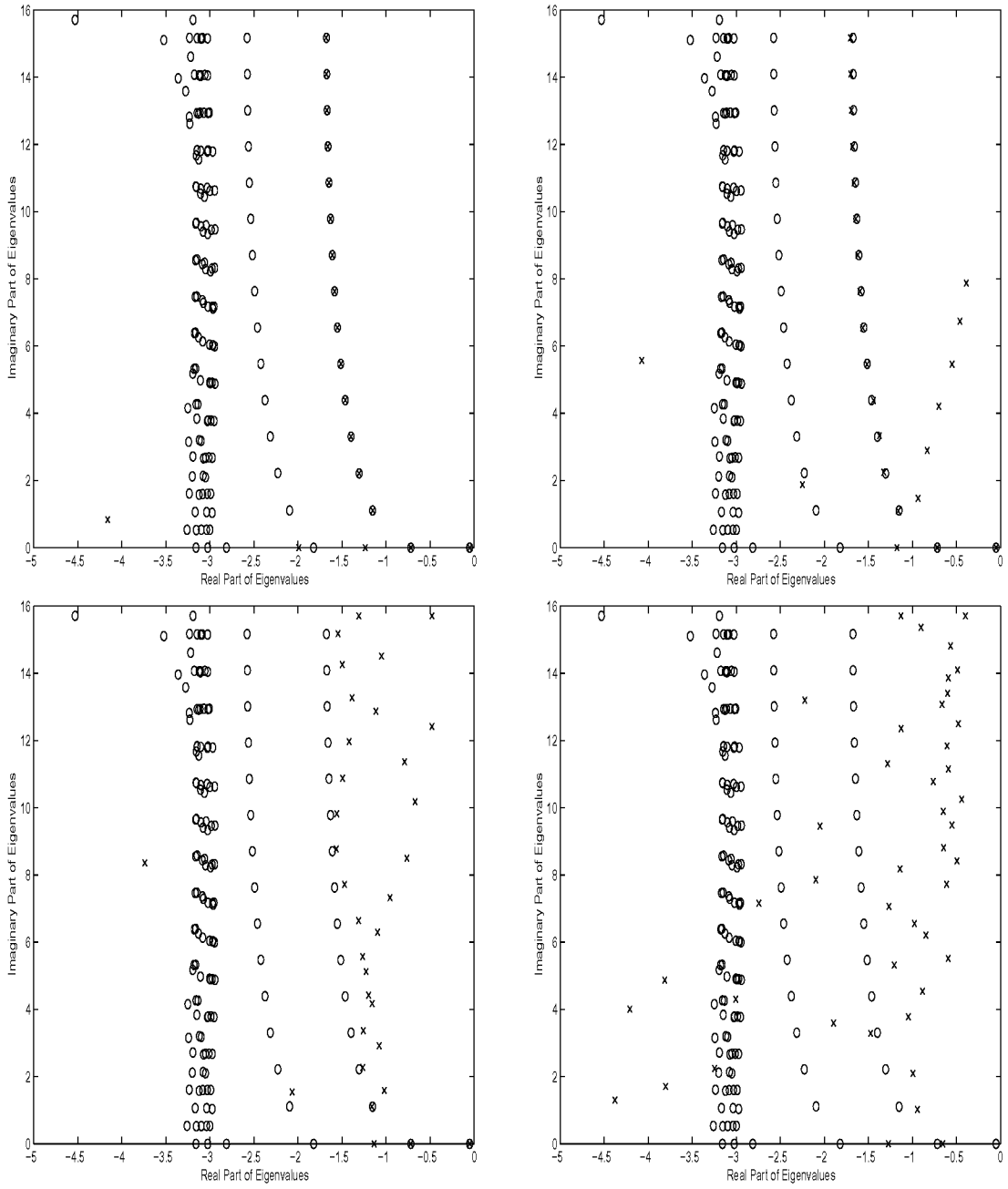

Figure 5: Original eigenvalues from VL code (∘) and eigenvalues from system ID model obtained using vortex strengths data on the wing and in the wake (×): (a) step angle of attack, (b) sharp edge gust, (c) swept gust, and (d) random case.

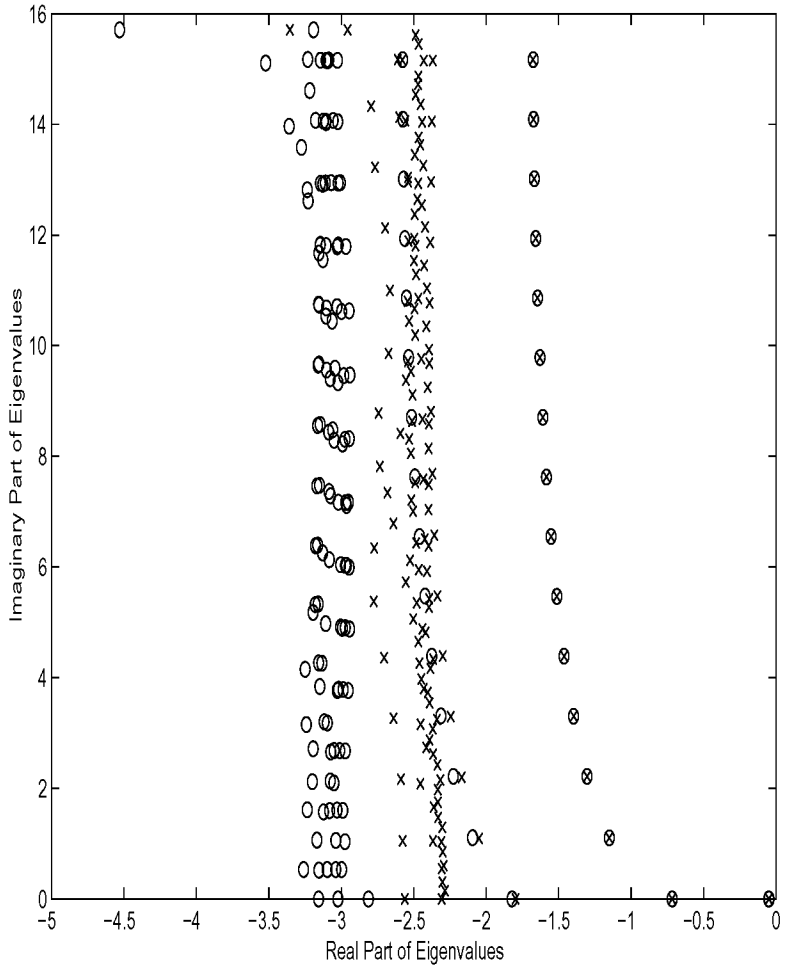

Figure 6: Original eigenvalues from VL code (∘) and eigenvalues from system ID model obtained using vortex strengths data on the wing and in the wake (×) for the random case when time series length is increased 10 times to 1000 time steps.

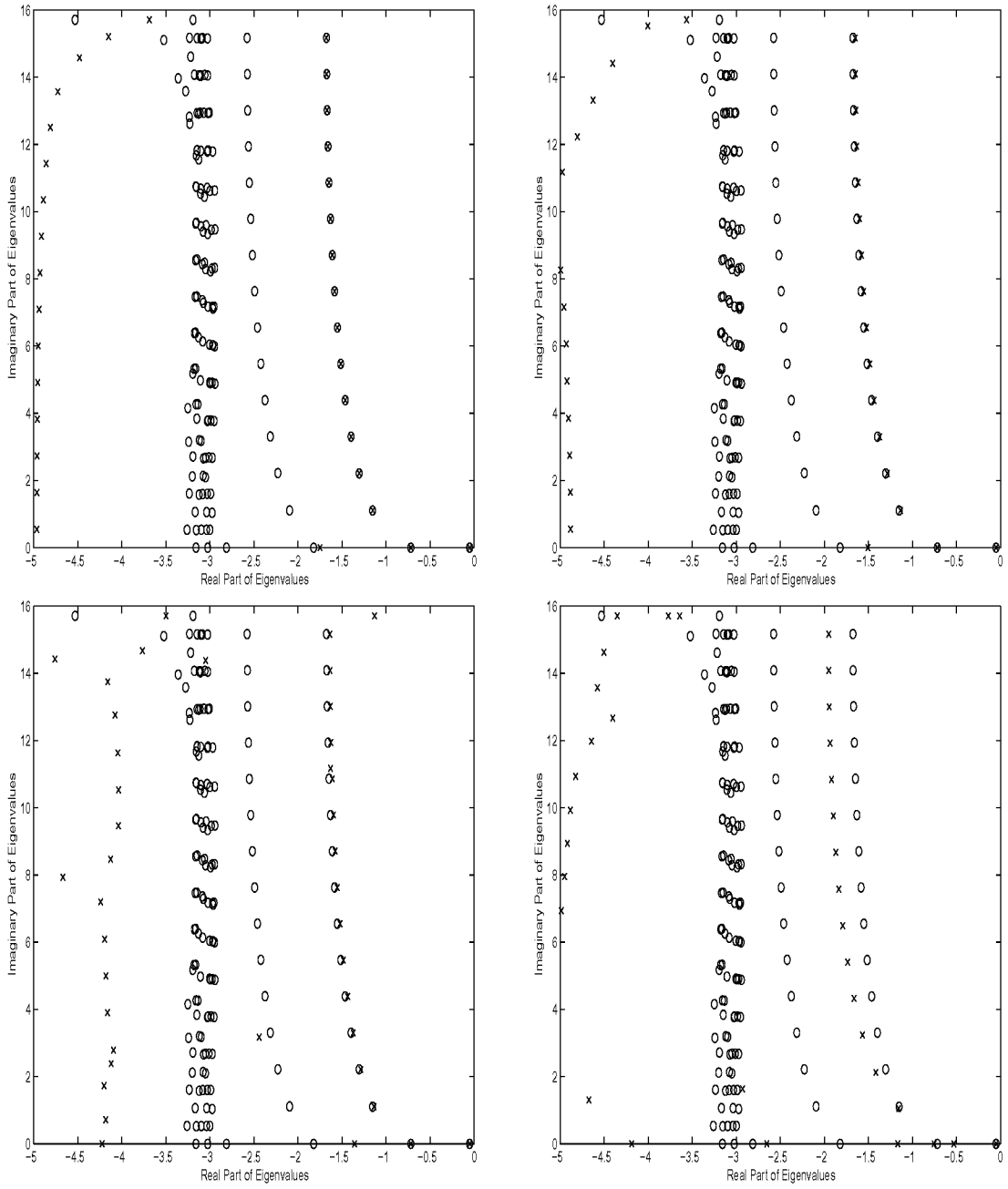

Figure 7: Original eigenvalues from VL code (∘) and eigenvalues from system ID model obtained using vortex strengths data on the wing only (×) : (a) step angle of attack, (b) sharp edge gust, (c) swept gust, and (d) random case.

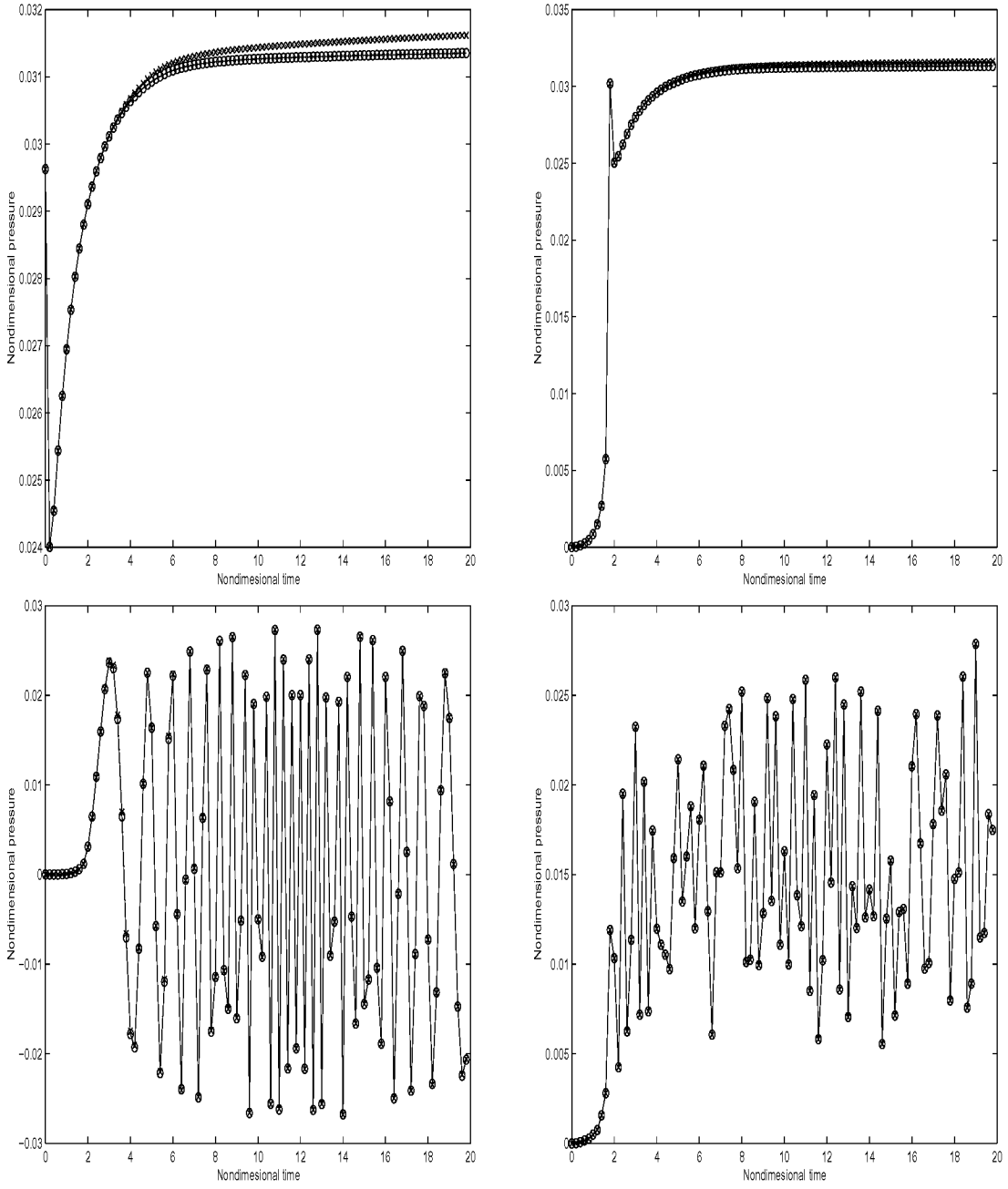

Figure 8: Time series of the pressure at the tip element. Original VL code data (solid line with ∘'s) and resulted time series from system ID model obtained using pressure on only 10 leading edge elements as input (dotted line with ×'s): (a) step angle of attack, (b) sharp edge gust, (c) swept gust, and (d) random case.

REPORT DOCUMENTATION PAGE

Form Approved
OMB No. 0704-0188

1. AGENCY USE ONLY *(Leave blank)*	2. REPORT DATE	3. REPORT TYPE AND DATES COVERED
	December 2001	Technical Memorandum

4. TITLE AND SUBTITLE
System Identification and Pod Method Applied to Unsteady Aerodynamics

5. FUNDING NUMBERS
WU 706-32-21-01

6. AUTHOR(S)
Deman Tang, Denis Kholodar, Jer-Nan Juang, and Earl H. Dowell

7. PERFORMING ORGANIZATION NAME(S) AND ADDRESS(ES)
NASA Langley Research Center
Hampton, VA 23681-2199

8. PERFORMING ORGANIZATION REPORT NUMBER
L-18119

9. SPONSORING/MONITORING AGENCY NAME(S) AND ADDRESS(ES)
National Aeronautics and Space Administration
Washington, DC 20546-0001

10. SPONSORING/MONITORING AGENCY REPORT NUMBER
NASA/TM-2001-211243

11. SUPPLEMENTARY NOTES
Tang, Kholodar, and Dowell: Duke University, Durham, NC; Juang: NASA Langley Research Center, Hampton, VA.

12a. DISTRIBUTION/AVAILABILITY STATEMENT
Unclassified-Unlimited
Subject Category 05 Distribution: Nonstandard
Availability: NASA CASI (301) 621-0390

12b. DISTRIBUTION CODE

13. ABSTRACT *(Maximum 200 words)*

The representation of unsteady aerodynamic flow fields in terms of global aerodynamic modes has proven to be a useful method for reducing the size of the aerodynamic model over those representations that use local variables at discrete grid points in the flow field. Eigenmodes and Proper Orthogonal Decomposition (POD) modes have been used for this purpose with good effect. This suggests that system identification models may also be used to represent the aerodynamic flow field. Implicit in the use of a systems identification technique is the notion that a relative small state space model can be useful in describing a dynamical system. The POD model is first used to show that indeed a reduced order model can be obtained from a much larger numerical aerodynamical model (the vortex lattice method is used for illustrative purposes) and the results from the POD and the system identification methods are then compared. For the example considered, the two methods are shown to give comparable results in terms of accuracy and reduced model size. The advantages and limitations of each approach are briefly discussed. Both appear promising and complementary in their characteristics.

14. SUBJECT TERMS
System Identification, Unsteady Aerodynamics, Proper Orthogonal Decomposition, State-Space Model Reduction.

15. NUMBER OF PAGES
29

16. PRICE CODE
A03

17. SECURITY CLASSIFICATION OF REPORT	18. SECURITY CLASSIFICATION OF THIS PAGE	19. SECURITY CLASSIFICATION OF ABSTRACT	20. LIMITATION OF ABSTRACT
Unclassified	Unclassified	Unclassified	UL